Phytochemistry 101 (2014) 23–31

Contents lists available at ScienceDirect

Phytochemistry

journal homepage: www.elsevier.com/locate/phytochem

7-Deoxyloganetic acid synthase catalyzes a key 3 step oxidation to form 7-deoxyloganetic acid in *Catharanthus roseus* iridoid biosynthesis

Vonny Salim [1], Brent Wiens, Sayaka Masada-Atsumi [2], Fang Yu, Vincenzo De Luca *

Department of Biological Sciences, 500 Glenridge Avenue, Brock University, St. Catharines, Ontario L2S 3A1, Canada

ARTICLE INFO

Article history:
Received 11 October 2013
Received in revised form 31 January 2014
Available online 1 March 2014

Keywords:
Madagascar Periwinkle
Catharanthus roseus
Apocynaceae
Secologanin biosynthesis
7-Deoxyloganetic acid synthase
Virus induced gene silencing
Functional characterization

ABSTRACT

Iridoids are key intermediates required for the biosynthesis of monoterpenoid indole alkaloids (MIAs), as well as quinoline alkaloids. Although most iridoid biosynthetic genes have been identified, one remaining three step oxidation required to form the carboxyl group of 7-deoxyloganetic acid has yet to be characterized. Here, it is reported that virus-induced gene silencing of 7-deoxyloganetic acid synthase (*7DLS*, *CYP76A26*) in *Catharanthus roseus* greatly decreased levels of secologanin and the major MIAs, catharanthine and vindoline in silenced leaves. Functional expression of this gene in *Saccharomyces cerevisiae* confirmed its function as an authentic 7DLS that catalyzes the 3 step oxidation of iridodial–nepetalactol to form 7-deoxyloganetic acid. The identification of CYP76A26 removes a key bottleneck for expression of iridoid and related MIA pathways in various biological backgrounds.

Introduction

Catharanthus roseus (Madagascar Periwinkle) is a member of the Apocynaceae family and remains the sole source of two monoterpenoid indole alkaloid (MIA) anticancer drugs, vinblastine and vincristine (van der Heijden et al., 2004). The therapeutic value of these compounds has led to extensive studies over the past 40 years to elucidate MIA biosynthetic pathways in the *C. roseus* model system. MIAs are derived from the central precursor, strictosidine that is formed through condensation of tryptamine and the iridoid secologanin (O'Connor and Maresh, 2006; El-Sayed and Verpoorte, 2007; Oudin et al., 2007).

Iridoids are monoterpenes usually characterized by their cyclopentane ring fused to a six-membered oxygen heterocycle and they are distributed in several plant families where they appear to serve as important defense compounds in plant–herbivore interactions. In addition, medicinal studies have reported their pharmacological activities against inflammation, as well as in liver and heart conditions (Dinda et al., 2007; Dinda et al., 2011; El-Sayed and Verpoorte, 2007). In many plant species, such as in *Lonicera japonica*, iridoids are found as major end products, while in others, they are further metabolized to produce different classes of alkaloids, such as MIAs in the Apocynaceae family and the quinoline alkaloids in members of the Rubiaceae. Despite the medicinal importance of these compounds, most of the genes responsible for iridoid and MIA biosynthesis have until recently been poorly characterized.

The early stages of iridoid biosynthesis (Fig. 1) involve the hydroxylation of geraniol (1) catalyzed by geraniol 10-hydroxylase (G10H or CYP76B6) (Collu et al., 2001), while 10-hydroxygeraniol oxidoreductase (Ikeda et al., 1991) catalyzes its further oxidation to the dialdehyde, 10-oxogeranial (5) (Fig. 1). Recently the iridoid synthase (IRS) gene product was shown to be involved in the cyclization step of the dialdehyde (5) to form *cis–trans*-nepetalactol that equilibrates with *cis–trans*-iridodial (6) under aqueous conditions (Geu-Flores et al., 2012). While it has been proposed that the cyclized product is further oxidized to form iridotrial (9) (Uesato et al., 1986), the gene(s) responsible for the oxidation steps leading to the formation of 7-deoxyloganetic acid (10) (Fig. 1, *7DLS*) have not been characterized. The 7-deoxyloganetic acid glucosyltransferase (*DLGT*) gene responsible for the formation of 7-deoxyloganic acid (11) has been functionally characterized from *C. roseus* (Asada et al., 2013). The substrate specificity of the recombinant DLGT for 7-deoxyloganetic acid (10) suggests this reaction takes place prior

* Corresponding author. Tel.: +1 905 688 5550x4554.
E-mail addresses: vs08to@badger.ac.brocku.ca (V. Salim), bw09ep@badger.ac.brocku.ca (B. Wiens), smasadaatsumi@nihs.go.jp (S. Masada-Atsumi), fyu0506@gmail.com (F. Yu), vdeluca@brocku.ca (V. De Luca).
[1] Present address: Biochemistry and Molecular Biology, Michigan State University, East Lansing, MI 48824-1319, United States.
[2] Present address: Division of Pharmacognosy, Phytochemistry and Narcotics, National Institute of Health Sciences, 1-18-1 Kamiyoga, Setagaya-ku, Tokyo 158-8501, Japan.

http://dx.doi.org/10.1016/j.phytochem.2014.02.009
0031-9422/

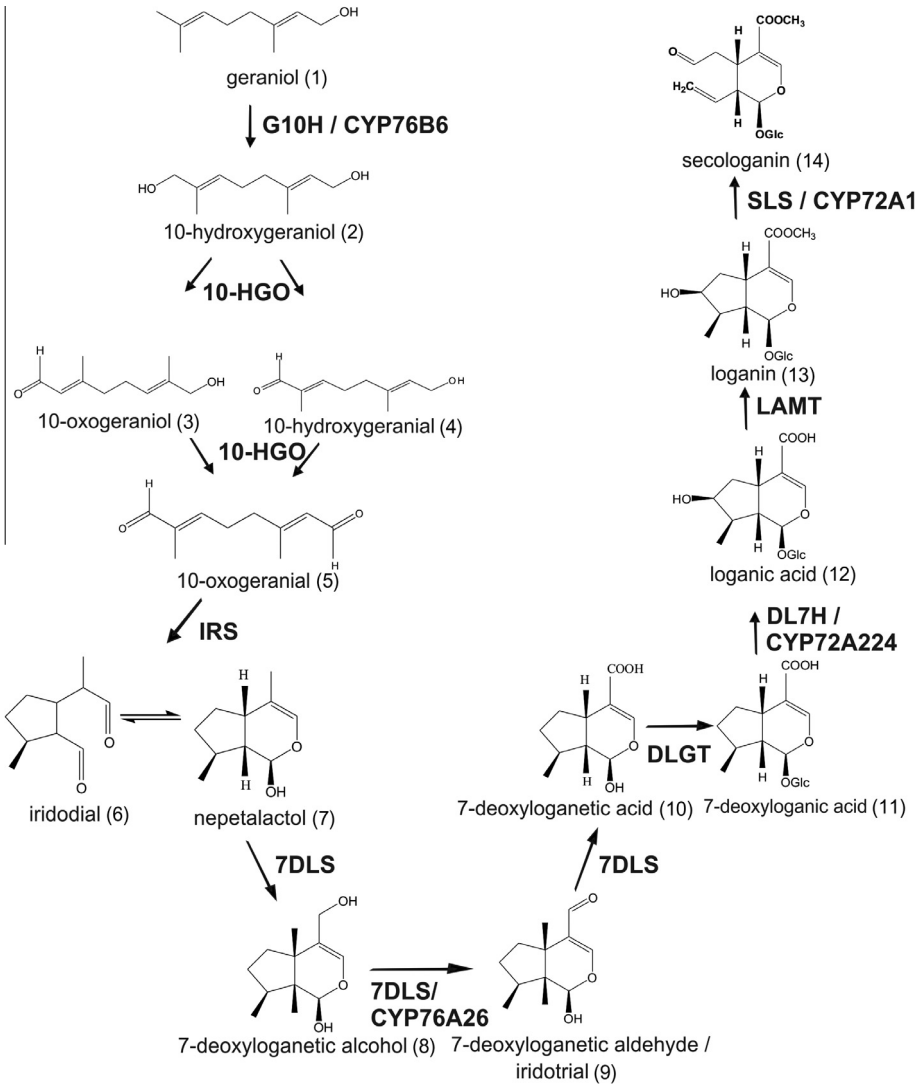

Fig. 1. Secologanin (14) biosynthesis in *Catharanthus roseus* includes three oxidation steps required to form 7-deoxyloganetic acid (10) from iridodial (6)–nepetalactol (7). Abbreviations: G10H: geraniol 10-hydroxylase, 10-HGO: 10-hydroxygeraniol oxidoreductase, IRS: iridoid synthase, *7DLS*: 7-deoxyloganetic acid synthase, DLGT: 7-deoxyloganetic acid glucosyltransferase, DL7H: 7-deoxyloganic acid 7-hydroxylase, LAMT: loganic acid *O*-methyltransferase, SLS: secologanin synthase.

to 7-hydroxylation and the recent functional characterization of Catharanthus 7-deoxyloganic acid 7-hydroxylase (DL7H, CYP72A224) corroborated its function to catalyze the hydroxylation of 7-deoxyloganic acid (11) to form loganic acid (12) (Salim et al., 2013). These results are supported by the preference of the next enzyme in the pathway, loganic acid *O*-methyltransferase (LAMT), for loganic acid (12) rather than 7-deoxyloganic acid (10) (Murata et al., 2008). The methylated product, loganin (13) is then further converted to yield secologanin (14) by secologanin synthase (CYP72A1) (Irmler et al., 2000) (Fig. 1). *In situ* hybridization studies showed that both IRS (Geu-Flores et al., 2012) and DLGT (Asada et al., 2013) are preferentially expressed in the internal phloem parenchyma cells of Catharanthus leaves, while LAMT and SLS (Guirimand et al., 2011; Murata et al., 2008) occurred preferentially in the leaf epidermis. Other studies with DL7H suggested that the 7-hydroxylase is also preferentially expressed within Catharanthus leaves than in the leaf epidermis (Salim et al., 2013). These results suggest that the 6 step biosynthesis of loganic acid (12) from geraniol (1) occurs in IPAP cells, while the terminal 2 steps to form secologanin (14) occur in the leaf epidermis.

The successful identification, cloning and functional characterization of DL7H (Salim et al., 2013) involved a bioinformatic search (Salim and De Luca, 2013) for homologous cytochrome P450 (CYP) candidate genes from the Phytometasyn website (www.phytometasyn.ca) which contains annotated express sequence tag databases of 7 plant species from the Apocynaceae family that make secologanin (14) and MIAs, one species from the Rubiaceae family that makes secologanin (14) and quinoline alkaloids, and one from the Caprifoliaceae family that makes secologanin (14). This search led to the identification of three candidate CYPs and virus induced gene silencing (VIGS) of each candidate was monitored for a decline in secologanin (14) levels as a result of gene silencing (Salim et al., 2013). The DL7H gene was identified in VIGS experiments, since significant amounts of its substrate 7-deoxyloganic acid (11) accumulated, while secologanin (14) levels declined sharply. This original screen established that a second candidate CYP (CYP76A26) might also be involved in the secologanin (14) pathway. The present study shows that VIGS silencing of CYP76A26 in Catharanthus plants triggers significant declines in secologanin (14) and MIA levels in silenced plants. Functional expression of this cytochrome P450 gene in yeast identified this CYP as 7-deoxyloganetic acid synthase that oxidizes nepetalactol (7) to form the carboxyl group of 7-deoxyloganetic acid (10) (Fig. 1). This discovery completes the characterization of the 8 genes required to form

secologanin (14) from geraniol (1) and should facilitate metabolic engineering efforts to produce iridoids or MIAs in plants or in heterologous systems such as yeast.

Results

Mining EST databases of secologanin (14) producing species for cytochrome P450 genes

Screening of annotated transcript databases (http://www.phytometasyn.ca/) from *Vinca minor*, *Rauwolfia serpentina*, *Tabernaemontana elegans*, *Amsonia hubrichtii*, *Cinchona ledgeriana* and from *L. japonica* that led to the identification of *CYP76A26*, *CYP72A224* (DL7H) and *CYP72A271* was performed as described previously (Salim et al., 2013; Salim and De Luca, 2013).

Virus-induced gene silencing of CYP76A26 alters the secologanin (14) contents of silenced Catharanthus plants

The usefulness of VIGS using a pTRV vector system (Burch-Smith et al., 2004) for gene identification has been demonstrated in previous studies that led to functional characterization of iridoid synthase (IRS) (Geu-Flores et al., 2012), iridoid glucosyltransferase, LAMT, SLS (Asada et al., 2013), and DL7H (Salim et al., 2013) that are all involved in secologanin (14) biosynthesis, as well as an *N*-methyltransferase involved in the 3rd to last step in vindoline biosynthesis (Liscombe and O'Connor, 2011). In the present study, use of this approach showed that silencing of CYP76A26 (Fig. 1, *7DLS*) resulted in a dramatic decrease in levels of secologanin (14) in *7DLS-vigs* silenced plants (*7DLS-vigs-1 and vigs-2*) compared to those found in control plants treated with empty vector (Fig. 2). As already described in previous studies (Geu-Flores et al., 2012; Asada et al., 2013; Salim et al., 2013; Liscombe and O'Connor, 2011), separate simultaneous silencing experiments of phytoene desaturase (PDS) were performed since the visible photobleaching produced was used to determine the appropriate timing for performing the analyses of *7DLS-vigs* silenced plants.

To confirm the suppression of the targeted transcripts, quantitative real-time PCR was performed to measure the silencing levels achieved in *7DLS-vigs* silenced plants. Plants infiltrated with *Agrobacterium tumefaciens* harboring *pTRV2–7DLS* showed >75% reduction in the level of *7DLS* transcripts compared with those harboring empty pTRV2 and mock treatments (Fig. 3A, P value < 0.05). While the suppression of *7DLS* expression (Fig. 3A) caused a 60% reduction in the abundance of secologanin (14) compared to untreated, empty pTRV2 and mock treatments (Fig. 3B), the mass signatures of iridoid intermediates (iridodial (6), nepetalactol (7) or other iridoids) were not detected in chromatograms. In contrast suppression of the last 3 steps in secologanin (14) biosynthesis resulted in the accumulation of the respective substrates for each reaction (Asada et al., 2013; Salim et al., 2013). As expected, plants suppressed for *7DLS* expression accumulated approximately 50% and 30% less of the major MIAs, catharanthine and vindoline, compared to untreated, empty pTRV2 and mock treatments, respectively (Fig. 3C).

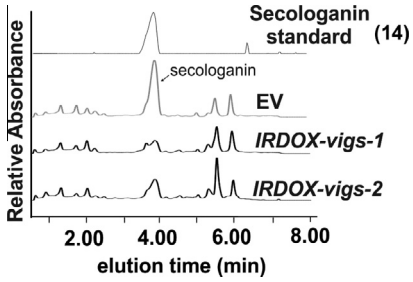

Fig. 2. VIGS of *7DLS* in *Catharanthus roseus* affects the levels of the major iridoid, secologanin (14). Selected UPLC-MS chromatogram of iridoid profile showing decreased level of secologanin (14) in VIGS plants when *7DLS* was silenced (*7DLS-vigs-1* and *2*) compared with empty pTRV2 vector-treated plants (EV).

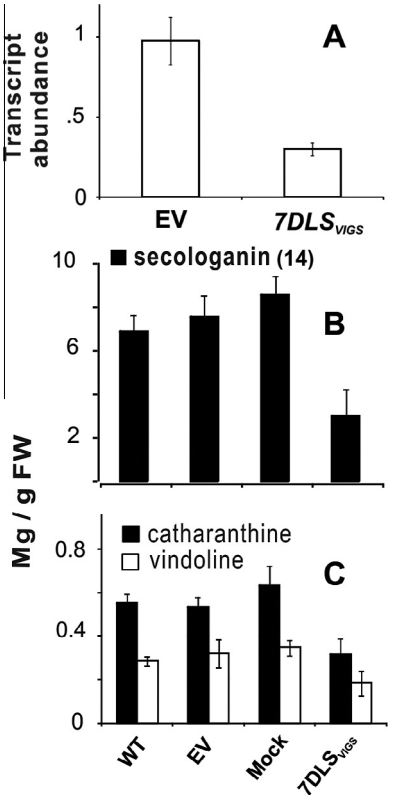

Fig. 3. *In planta* silencing of *7DLS* causes a decline in secologanin (14), catharanthine and vindoline levels. (A) Real-time quantitative PCR analysis (qPCR) of plants infiltrated with *Agrobacterium tumefaciens* harboring pTRV2–*7DLS* constructs compared with empty pTRV2 vector controls (EV). qPCR was performed on RNA extracted from individual half leaf pairs of VIGS-treated plants when the other half was used for metabolite extraction. (B) Quantification of secologanin (14) and (C) major MIAs, catharanthine and vindoline in *Catharanthus roseus* plants infiltrated with *Agrobacterium tumefaciens* harboring pTRV2–*7DLS* compared with EV. The data represents the mean ± standard error of at least eight biological replicates for metabolites or transcript levels prepared from individual plants infiltrated with *A. tumefaciens* containing each construct. Significance differences were considered with P values <0.05 by Student's t-test for the transcript analysis and metabolite contents of EV-treated plants and each silenced plant. Metabolite analysis of wild type, EV, and VIGS infected plants demonstrated that MIA production was impaired when secologanin (14) biosynthesis was suppressed by silencing iridoid biosynthetic gene *7DLS*.

Functional characterization of 7DLS

To validate the identification of CYP76A26, an *in vivo* assay was performed by using an engineered dual expression yeast system, pESC-Leu2d as previously described (Salim et al., 2013). After gene and protein expression was induced by the addition of galactose, gas chromatography-mass spectrometry analysis of yeast cultures expressing *7DLS* showed that they consumed most of the nepetalactol (7) (RT = 28.69 min), while no significant depletion of this substrate occurred in yeast cultures transformed with empty pESC-Leu2d (Fig. 4A). The consumption of nepetalactol (7) in the yeast cultures expressing *7DLS* triggered our search to find the product of the reaction by comparison of mass spectra between yeast cultures containing *7DLS* protein and the empty vector control. Trace levels of a product with the correct mass of iridotrial (9) was detected (RT 31.87 min) in yeast cultures expressing *7DLS*, but not in control cultures harboring the empty pESC-Leu2d

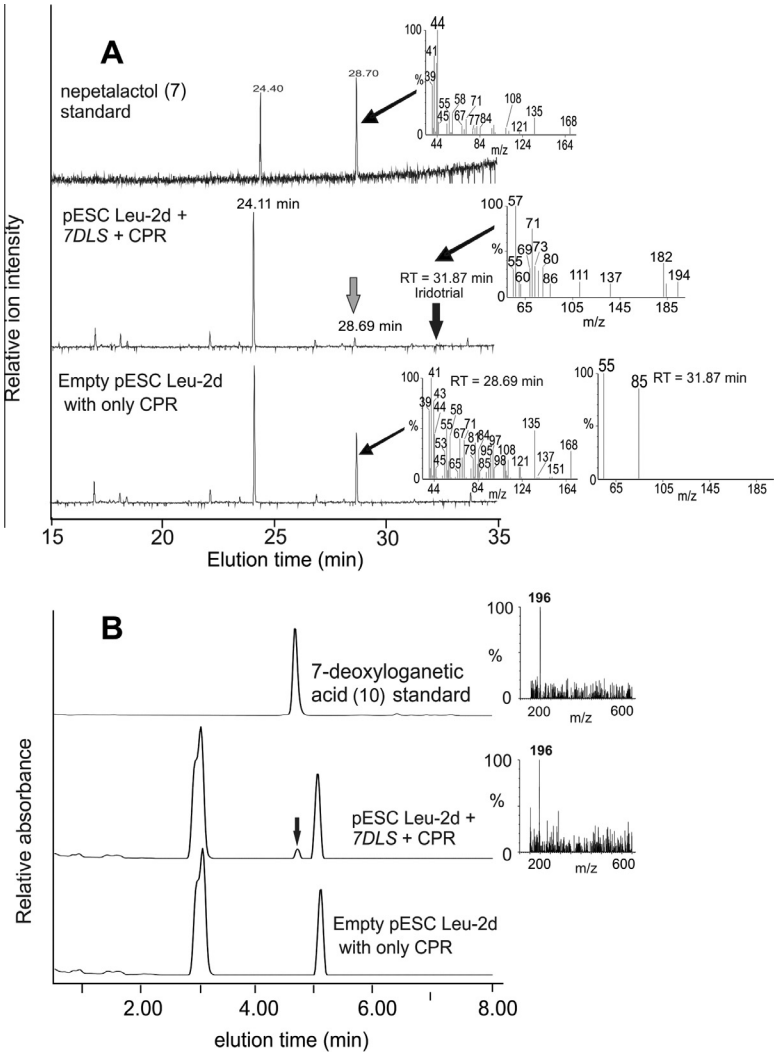

Fig. 4. Recombinant *7DLS* expressing yeast cultures biotransform nepetalactol (7) to 7-deoxyloganetic acid (10). (A) Selected GC–MS chromatogram of yeast cell cultures expressing *7DLS*, or empty pESC-Leu2d vector supplemented with nepetalactol (RT = 28.69 min). *In vivo* assay of yeast cells expressing *7DLS* showed that the nepetalactol (7) was consumed compared with the empty vector control. The reduction of nepetalactol (7) (grey arrow; RT = 28.69 min) in the yeast cells expressing *7DLS* is also matched by the appearance of traces of the intermediate iridotrial (9) (black arrow; RT = 31.87 min) based on mass spectra difference between yeast cells expressing *7DLS* and harboring empty vector. The additional peak (RT = 24.11 min) occurring in the GC is phenethyl alcohol that typically occurs in yeast extracts. (B) UPLC-MS chromatogram of yeast cell cultures expressing 7DLS, or empty pESC-Leu2d vector supplemented with nepetalactol (7) (not detected by UPLC-MS). Iridoid analysis of the yeast cells expressing 7DLS (pESC-Leu2d-*7DLS* + CPR) showed the appearance of 7-deoxyloganetic acid (10) (black arrow, RT = 4.68 min, m/z = 196), whereas the empty vector expressing yeast (pESC-Leu2d + CPR) produced no product. The retention time and mass spectra of product was compared with authentic 7-deoxyloganetic acid (RT = 4.68 min). Mass spectra of compound identified as nepetalactol (7) (RT = 28.69 min) and 7-deoxyloganetic acid aldehyde, iridotrial (9) (RT = 31.87 min) previously shown in GC–MS analysis were not detectable in UPLC-MS run. The additional peaks (RT = 3 and 5.2 min) are uncharacterized metabolites with m/z 120, UV max 217 and 328 nm; m/z 162, UV max 222 and 280 nm, respectively) as a result of yeast metabolism during biotransformation which were detected in both 7DLS and empty vector expressing lines.

vector (Fig. 4A). This yeast biotransformation assay suggested that *7DLS* expressing cultures might be converting nepetalactol (7) to undetermined products that could not be detected with this GC method via iridotrial (9). When biotransformation products were analyzed by UPLC-MS, 7-deoxyloganetic acid (10) (RT = 4.68 min, m/z = 196) (Fig. 4B) could be clearly detected in 7DLS expressing cultures, but not in the empty vector control line.

The enzyme activity of *7DLS* was also examined by preparing microsomes from *7DLS* expressing yeast. Analyses by GC–MS showed that microsomes did produce trace levels of iridotrial (9) in the presence of NADPH (Supplementary Fig. S1A) similar to those obtained in biotransformation experiments (Fig. 4A). When reaction products were analyzed by UPLC-MS, microsomes expressing *7DLS* catalyzed the successive oxidation of nepetalactol (7) to generate 7-deoxyloganetic acid (10) (RT = 4.68 min, m/z = 196) (Fig. S1B) suggesting that CYP76A26 is responsible for the three step oxidation required to form the carboxyl group of 7-deoxyloganetic acid (10) (Fig. 1). The amount of 7-deoxyloganetic acid (10) being produced in typical assays was quite variable (8–24% conversion of the original nepetalactol (7) provided). The difficulties encountered with this assay might be due to the instability of the initial substrate, as well as of the reaction intermediates being produced. The enzyme was not able to accept a variety of other possible substrates, including geraniol (1), 10-hydroxygeraniol (2), 10-oxogeranial (3), citral, and nerolidol. This result also confirms that cyclization of monoterpenes needs to take place before this series of oxidations and the other enzyme reactions that ultimately lead to the formation of secologanin (Fig. 1).

Organ specificity of 7DLS expression and non-epidermal enrichment

Analyses of *7DLS* transcript levels by quantitative real-time PCR (qPCR) showed that its expression profile was consistent with those obtained with other steps in iridoid biosynthesis

(Asada et al., 2013; Salim et al., 2013). While relative expression of *7DLS* was highest in the youngest leaves (Fig. 5A, leaf pairs 1 and 2), it was also well expressed in older leaves (Fig. 5A, leaf pairs 3, 4 and 5), in stems and to a slightly lower extent in flower buds and roots. These data suggest that iridoid biosynthesis may be taking place in all organs and over a broader range of plant development than the more tightly controlled timing that restricts the biosynthesis and accumulation of MIAs to younger leaves (Roepke et al., 2010) and to root meristems (Laflamme et al., 2001; Magnotta et al., 2007). Overall, the comparison of *7DLS* expression with other iridoid biosynthetic genes such as *DL7H*, *LAMT*, and *SLS* showed a coordinated expression profile that is consistent with its involvement in iridoid and MIA biosynthesis.

The enrichment of iridoid or MIA biosynthetic genes in leaf epidermis cells has been previously tested by analyzing epidermis-enriched RNAs extracted by carborundum abrasion (Murata et al., 2008; Salim et al., 2013) and by comparing this enrichment to that found in RNA obtained from whole leaves. Expression analysis of *7DLS* in *C. roseus* leaves indicates that this CYP is 4-fold more abundant in the whole leaf than in the epidermis (Fig. 5B). Transcript levels of *G10H*, *IRS*, *DLGT* and *DL7H* were also at least 4-fold more abundant in whole leaves than in the epidermis while expression of *LAMT* and *SLS* was enriched several fold in the leaf epidermis (Fig. 5B). These results are entirely consistent with the previously reported spatial expression pattern for geraniol synthase (Simkin et al., 2013), *G10H* (Burlat et al., 2004), *IRS* (Geu-Flores et al., 2012), *DLGT* (Asada et al., 2013), *DL7H* (Salim et al., 2013) that were preferentially expressed inside leaf internal phloem parenchyma (IPAP) cells, while *LAMT* (Murata et al., 2008; Guirimand et al., 2011), and *SLS* transcripts were restricted to leaf epidermal cells (Irmler et al., 2000). These data together with enrichment of the methylerythritol phosphate (MEP) pathway (Burlat et al., 2004) in IPAP cells suggest their central role in the assembly of loganic acid, before being transported to epidermal cells to be converted to secologanin by LAMT and SLS.

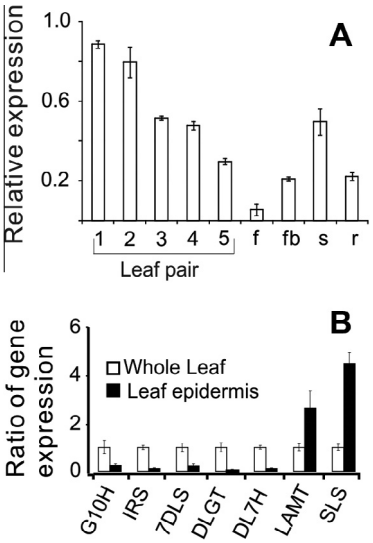

Fig. 5. *7DLS* gene expression in different Catharanthus organs, cell types and developmental stages. (A) The transcript level of *7DLS* in various organs and leaf ages of *Catharanthus roseus* were analyzed by quantitative real-time PCR. The data are displayed as a relative expression compared to the housekeeping gene, 60S ribosomal *RPP0C* transcript. Error bars represent standard deviation of three biological replicates each performed with 3 technical replicates. The expression pattern of *7DLS* is similar with the expression of other iridoid biosynthetic genes, *DL7H*, *LAMT*, and *SLS*, as well as the distribution of secologanin (14) contents that were previously reported (Asada et al., 2013; Salim et al., 2013). (B) Epidermis enriched transcript analysis shows that *7DLS* is preferentially expressed within the leaves, similar to the patterns obtained with geraniol 10-hydroxylase (*G10H*), iridoid synthase (*IRS*), 7-deoxyloganetic acid glucosyltransferase (*DLGT*) and 7-deoxyloganic acid 7-hydroxylase (*DL7H*). In contrast the terminal pathway reactions, loganic acid *O*-methyltransferase (*LAMT*) and secologanin synthase (*SLS*) are preferentially expressed in leaf epidermal cells.

Discussion

Functional characterization of the last cytochrome P450 gene involved in the assembly of secologanin (14)

In order to complete our understanding of the complexity of plant secondary metabolic pathways in *C. roseus*, more biosynthetic genes involved in the formation of MIAs still need to be isolated and various large-scale transcriptomic projects have recently facilitate their discovery (Facchini et al., 2012; Xiao et al., 2013; Góngora-Castillo et al. 2012a,b; Van Moerkercke et al., 2013). In this study, candidate MIA biosynthetic genes were obtained by probing annotated databases from a recent large-scale trancriptome sequencing project of over 70 medicinal plants that produce various valuable secondary metabolites (http://www.phytometasyn.ca/) (Facchini et al., 2012; Xiao et al., 2013). Among these the transcriptomes of six Apocynaceae family MIA producing plants (*C. roseus*, *V. minor*, *R. serpentina*, *T. elegans*, *A. hubrichtii*, one quinoline alkaloid accumulating plant, (*C. ledgeriana* from the Rubiaceae family) and one species that only produces secologanin, (*L. japonica* from the Caprifoliaceae family) (Kawai et al., 1988) have been obtained and annotated. As the Apocynaceae members share the same central pathways for the biosynthesis of various MIAs, the orthologous genes involved in the MEP, and iridoid pathways were represented in all these species. The methodology of searching for novel biosynthetic genes from *C. roseus* based on comparisons among Apocynaceae datasets has been successfully applied for identification and functional characterization of DL7H (Salim et al., 2013), a cytochrome P450 monooxygenase involved in the 3rd to last step in secologanin (14) biosynthesis (Fig. 1) in Catharanthus. This approach to mining such datasets is becoming more common in the discovery process for iridoid and MIA pathway gene discovery (Salim et al., 2013; Geu-Flores et al., 2012; Liscombe and O'Connor, 2011).

The present report highlights the discovery of another Catharanthus CYP, 7-deoxyloganetic acid synthase, which adds to several other CYP genes known to carry out reactions in iridoid and MIA biosynthesis. These include *G10H* (Collu et al., 2001), *DL7H* (Salim et al., 2013), *SLS* (Irmler et al., 2000; Mizutani and Sato, 2011), *T16H* (Schröder et al., 1999) and *T19H* (Giddings et al., 2011). In this study, the bioinformatic strategy described narrowed down the candidate genes to be studied and virus-induced gene silencing (VIGS) was essential to further assist in gene identification and functional characterization (Figs. 2 and 3) . The usefulness of VIGS for gene functional analysis in *C. roseus* has been demonstrated such as in identification of the *N*-methyltransferase involved in the 3rd to last step in vindoline biosynthesis (Liscombe and O'Connor, 2011) and for the recent identification the remaining secologanin (14) pathway steps, *IRS* (Geu-Flores et al., 2012), *DLGT* (Asada et al., 2013) and *DL7H* (Salim et al., 2013). During the screening process to investigate candidate CYPs for their involvement in iridoid or MIA biosynthesis, silenced CYP76A26 exhibited reduced levels of secologanin (14) and MIA accumulation in silenced plants (Figs. 2 and 3) and this pattern was usually observed when other iridoid biosynthetic genes were suppressed (Asada et al., 2013). Although the silencing of this CYP does not show the accumulation of its substrate, this effect might be expected due to the limitations in detection of monoterpene precursors by UPLC-MS. In addition, *7DLS* expressing yeast converts the substrate, nepetalactol (7) to 7-deoxyloganetic acid (10) via iridotrial (9) in a three step oxidation (Figs. 4 and 5 and Fig. S1)

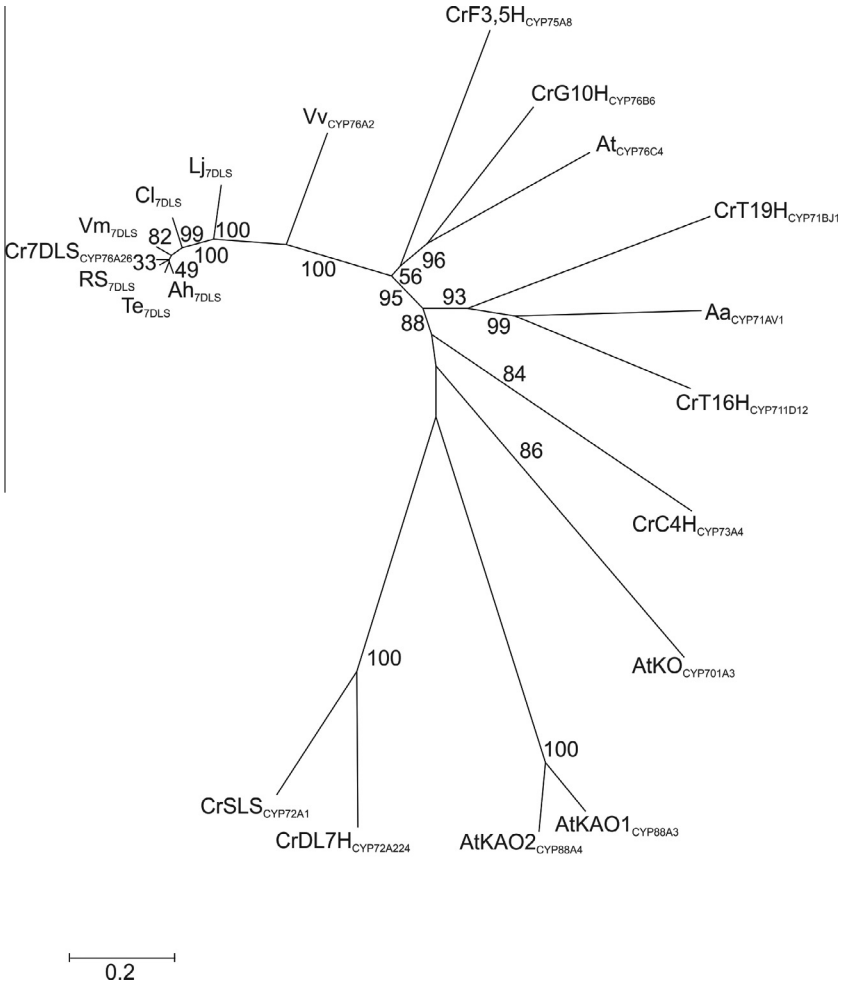

Fig. 6. Phylogenetic relationships among selected cytochrome P450s to *7DLS* from *Catharanthus roseus*. A phylogenetic tree was generated using the neighbor joining algorithm based on a comparison of the amino acid sequences using the ClustalW program. The scale bar of 0.2 indicates to a 20% change and the number shown next to the branches are the percentage of replicate trees in which the related taxa clustered together in the bootstrap test with 10,000 replicates. The accession numbers are: KF591593 (*Catharanthus roseus*, Cr*7DLS*-7-deoxyloganetic acid synthase); KF591587 (*Lonicera japonica*, Lj*7DLS*-7-deoxyloganetic acid synthase); KF591588 (*Cinchona ledgeriana*, Cl*7DLS*-7-deoxyloganetic acid synthase-like); KF591589 (*Amsonia hubrichtii*, Ah*7DLS*-7-deoxyloganetic acid synthase-like); KF591590 (*Rauwolfia serpentina*, Rs*7DLS*-7-deoxyloganetic acid synthase -like); KF591591 (*Tabernaemontana elegans*, Te*7DLS*-7-deoxyloganetic acid synthase -like); KF591592 (*Vinca minor*, Vm*7DLS*-7-deoxyloganetic acid synthase -like); AJ251269 (*Catharanthus roseus*, CrG10H-CYP76B6-geraniol 10-hydroxylase); L10081 (*Catharanthus roseus*, CrSLS-CYP72A1-secologanin synthase); KF415115 (*Catharanthus roseus*, CrDL7H-CYP72A224-7-deoxyloganic acid 7-hydroxylase); DQ315671 (*Artemisia annua*, AaCYP71AV1-amorpha-4,11-diene oxidase); AF047719 (*Arabidopsis thaliana*, AtKO-CYP701A3-ent-kaurene oxidase); AF318500 (*Arabidopsis thaliana*, AtKAO1-CYP88A3-ent-kaurene oxidase); AF318501 (*Arabidopsis thaliana*, AtKAO2-CYP88A4-ent-kaurene oxidase); NM_130117 (*Arabidopsis thaliana*, AtG8,9-OH-CYP76C4-geraniol 8-hydroxylase, geraniol 9-hydroxylase); Z32563 (*Catharanthus roseus*, CrC4H-CYP73A3-cinnamate 4-hydroxylase); HQ901597 (*Catharanthus roseus*, CrT19H-CYP71BJ1-tabersonine 19-hydroxylase); FJ647194 (*Catharanthus roseus*, CrT16H-CYP71D12-tabersonine 16-hydroxylase); AJ011862 (*Catharanthus roseus*, CrF3,5H-CYP75A8-flavonoid 3′,5′-hydroxylase); XP_002283772 (*Vitis vinifera*, VvCYP76A2-unknown protein).

which confirms its enzymatic activity in catalyzing successive oxidations. Although *7DLS* belongs to the same CYP76 family as *G10H* (CYP76B6), the substrate specificity of CYP76A26 for nepetalactol (7) shows the distinct properties of this enzyme in catalyzing a successive three step oxidation compared to *G10H* (CYP76B6) that accepts a broader range of substrates including geraniol, its oxidized derivative, nerol, and flavonoids (Höfer et al., 2013; Sung et al., 2011).

The gradual decrease of *7DLS* transcripts with leaf development is consistent with the expression patterns of other iridoid pathway genes such as *DL7H*, *LAMT*, and *SLS* in relation to the accumulation patterns of secologanin (14), catharanthine, and vindoline in this organ (Fig. 5A) (Asada et al., 2013). The detection of *7DLS* transcripts in whole leaf rather than epidermal cells could be predicted from the IPAP cell preferred expression of IRS (Geu-Flores et al., 2012) that makes the nepetalactol (7) substrate required for the 7DLS reaction and 7-deoxyloganetic acid glucosyltransferase that accepts the 7DLS reaction product (Asada et al., 2013). While the carborundum abrasion technique again demonstrated its use to identify preferentially expressed genes in the leaf epidermis, *in situ* hybridization studies to localize *7DLS* expression to IPAP cells are required to confirm these results.

Phylogenetic analysis

Phylogenetic analysis of *7DLS* sequences found in the Phytometasyn databases showed them to have the highest amino acid sequence identity to *CYP76A2* from *Vitis vinifera* (58%) whose biochemical function remains to be discovered. Interestingly, Catharanthus *7DLS* sequence (*Cyp76A26*) had lower amino acid sequence identities with *Catharanthus G10H* (39%, *CYP76B6*; Collu et al., 2001) and with Arabidopsis *CYP76C4* (36%; Höfer et al., 2013) that also shows a modified geraniol hydroxylase activity to that of *G10H*. Inspection of the Phytometasyn databases showed the presence of *CYP76A26* homologs in all secologanin producing species whose amino acid identities ranged from 76%

in *L. japonica* to 94% in *R. serpentina*. This phylogenetic analysis (Fig. 6) clearly demonstrates the distinct and separate grouping of 7-deoxyloganetic acid synthase-like genes from *C. roseus*, *V. minor*, *A. hubrichtii*, *R. serpentina*, *C. ledgeriana* and *L. japonica* from other *C. roseus* CYPs that have been functionally characterized [flavonoid 3',5'-hydroxylase (*CYP75A8*) (Kaltenbach et al., 1999), cinnamate 4-hydroxylase, (*C4H*; *CYP73A4*) (Hotze et al., 1995), tabersonine 16-hydroxylase, (*T16H*; *CYP71D12*) (Schröder et al., 1999), and tabersonine 19-hydroxylase, (*T19H*; *CYP71BJ1*) (Giddings et al., 2011]. Interestingly, the 7-deoxyloganetic acid synthase-like genes also group separately from other CYPs that catalyze three step oxidations, such as *CYP71AV1* involved in artemisinin biosynthesis (Teoh et al., 2006) and ent-kaurene oxidase involved in gibberellic acid biosynthesis, *CYP701A3*, *CYP88A3* and *CYP88A4* (Helliwell et al., 1998; Helliwell et al., 2001) (Fig. 6).

The prospect of metabolic engineering to increase the production of MIAs with the completion of secologanin biosynthesis pathway

The involvement of *7DLS* (CYP76A26) in successive oxidation of iridodial–nepetalactol (7) to 7-deoxyloganetic acid (10) (Fig. 4B) is clearly significant, as it is the last gene that remained to be characterized to complete the secologanin (14) biosynthesis pathway. The oxidations involved may include the formation of the alcohol, the aldehyde and the carboxylic acid (Fig. 1) by a mechanism that remains to be elucidated since our studies did not reveal the formation of an alcohol intermediate and only trace levels of the putative iridotrial (9) were found in yeast feeding studies (Fig. 4A) and in microsomal enzyme assays (Fig. S1). In the case of artemisinin biosynthesis, the functional characterization of *CYP71AV1*, that also catalyzes successive oxidations from amorpha-4,11-diene to form artemisinic acid (Teoh et al., 2006), led to the efforts to engineer a yeast strain that can supply this anti-malarial drug more efficiently (Ro et al., 2006; Ro et al., 2008). The availability of the *7DLS* sequence now allows engineering of this gene with other iridoid biosynthetic genes to provide more insight into secologanin (14) biosynthesis and in efforts to engineer the entire secologanin (14) pathway in plants, yeast or other microbial hosts.

Experimental

Plant materials

C. roseus (L.) Don cv. Little Delicata seeds were grown in the greenhouse under a 16:8 Light: Dark photoperiod at 28 °C. For VIGS treatments, seedlings were grown in 50 well trays for 4 weeks after seed germination or until they produce at least two true leaf pairs.

Chemicals

Nepetalactol (7) was synthesized by Professor John Pickett at Rothamsted, UK and was kindly provided by Professor Sarah O'Connor from the John Innes Center, while 7-deoxyloganetic acid (10) was provided by Professor Hajime Mizukami, Nagoya City University, Japan.

VIGS vectors containing 7DLS

A fragment of 319 bp from the 7-deoxyloganetic acid synthase candidate gene was amplified by PCR with Ex-Taq polymerase (Takara), *C. roseus* cDNA, primers VIGS-*7DLS*-Fw-5′- TGGCGTTAAACCACAAGATA-3′ and VIGS-*7DLS*-Rv-5′- ACGAAGACAAGGAACAATCA-3′ and inserted into the EcoRI site of pGEMT-Easy vector (Promega). The *7DLS* fragment was subcloned into the EcoRI site between the CaMV 35S promoter (2x35S) and NOS terminator of the pTRV2 vector in the correct orientation which was verified by sequencing. The assembly of pTRV1 and pTRV2 vectors were previously described (Dinesh-Kumar et al., 2003). VIGS was performed following protocols as described previously (Liscombe and O'Connor, 2011; De Luca et al., 2012). After 3 weeks, leaf material was harvested for metabolite analysis and RNA extractions to measure transcript levels were performed according to Salim et al. (2013).

Expression of 7DLS in yeast

The open reading frame (ORF) of CYP76A26 (Genbank™ accession no KF591593), assigned by the P450 nomenclature committee (D.R. Nelson), was amplified by PCR using High-Fidelity Phusion DNA polymerase (New England Biolabs) and gene specific primers, ORF-*7DLS* Fw-5′- TACAGCGGGCCCAGGATGGCGACCATCACTTTC-3′ with *ApaI* site (underlined) and ORF-*7DLS*-Rv-5′- GCGCGTCGACGATATGAACTCTCTTCTTAG-3′ with *SalI* site (underlined) and cloned via the pGEMT-Easy vector (Promega) into the pESC-Leu2d yeast dual expression vector (Stratagene) behind the Gal-1 promoter (Ro et al., 2008). This vector already contains an insert of *C. roseus* NADPH-cytochrome P450 reductase (CPR) (Genbank™ accession no X69791.1) behind the Gal-10 promoter as previously described (Salim et al., 2013).

The plasmid containing *7DLS* was introduced into the *Saccharomyces cerevisiae* strain MKP-0 via the standard polyethylene glycol–lithium acetate procedure (Gietz et al., 1992). The corresponding empty vector with only CPR was also introduced into this yeast strain. Transformants were selected on SD-Leu dropout medium with 2% glucose as a carbon source and induced by SG-Leu dropout medium containing 2% galactose, as described previously (Ro et al., 2002).

For *in vivo* assay in yeast, late-log phase yeast cells (50 mL) were harvested by centrifugation at 1000*g* after induction and were subsequently suspended in Tris–EDTA buffer (25 mL, pH 7.5) containing 0.2 mM nepetalactol (7) dissolved in 0.4% tetrahydrofuran (THF) in H_2O. The yeast culture was incubated at 28 °C for 24 h in a 150-rpm shaker. After cells were removed by centrifugation, the medium was extracted with an equal volume of CH_2Cl_2. The CH_2Cl_2 layer was isolated, aliquoted equally into two tubes and dried down under a stream of gaseous N_2. The sample in the first tube was dissolved in CH_2Cl_2 (0.5 mL) and analyzed by GC–MS, while the second tube was dissolved in MeOH (200 μL) for UPLC-MS analysis.

Yeast microsomes were prepared as described in Pompon et al. (1996) using the high density procedure and the total microsomal protein content was measured (Bradford, 1976). *7DLS* activity was determined in a reaction mixture (0.2 mL) containing microsomal protein (480 μg), 1 mM NADPH, 4 mM dithiothreitol and the reaction was initiated by addition of 200 μM nepetalactol (7) in 0.4% THF in H_2O and incubated for 120 min at 30 °C. Assays containing boiled microsomes or lacking NADPH served as negative controls. The reaction was terminated by adding CH_2Cl_2 (500 μL). After vortexing the mixture followed by centrifugation at 14,000*g* for 20 min, the CH_2Cl_2 phase was isolated and half of the sample was analyzed by GC–MS. The other half was dried down under a stream of gaseous N_2, dissolved in MeOH (200 μL) for UPLC-MS (Roepke et al., 2010) analysis to detect the reaction product, 7-deoxyloganetic acid (10).

Metabolite analysis by GC–MS and UPLC-MS

GC–MS analysis was performed with Perkin Elmer AUTOSYSTEM XL GC–MS with with TurboMass Gold mass spectrometer, equipped with an autosampler. Samples (1 μL) were injected into the injection port held at 200 °C, utilizing a flow rate of

1.2 ml/min of He. The column (VF-WAX ms, Varian Inc., 30 m x 0.25 mm × 0.25 μm) was heated according to the following oven program: held at 60 °C for 2 min, then ramped up at 4.0 °C/min to 245 °C, and held for 10 min. The mass spectrometer (source temperature set to 150 °C and GC inlet line set to 175 °C) acquired data under the following conditions: after a 2 min solvent delay, total ion scans were initiated in EI + ionization mode, from $m/z = 35$ to $m/z = 350$ at 2.5 scans per second. Total ion counts and masses were called by the software according to the NIST databases (NIST 98) installed in the system, and retention times were compared to authentic standards.

UPLC-MS analysis for iridoid analysis in enzyme assays were performed as described in Asada et al. (2013) with mass spectrometer operated with an electrospray ionization source of negative ionization (7-deoxyloganetic acid (10), m/z 196, RT = 4.68 min). MIAs extracted from VIGS-treated plants were separated as described in Roepke et al. (2010) for detection of catharanthine and vindoline. Iridoids from VIGS treatment were analyzed as described in Asada et al. (2013) with mass spectrometer set with positive ionization mode for analysis of secologanin (14) level (m/z 389, RT = 3.88 min).

Quantitative real-time PCR (qPCR)

Preparation of total RNAs from various tissues of *C. roseus* and subsequent first-strand cDNA synthesis were performed according to Salim et al., 2013. The gene expression level of CYP76A26 in various tissues and VIGS samples was analyzed by qPCR using primers, RT-*7DLS* -Fw-5′-AGAACTTCTCCGAAACCCAC-3′ and RT-*7DLS*-Rv-3′-CTAAGCGTCTCCTTTACAAC-3′. The 60s ribosomal RPP0C gene was chosen as a housekeeping gene and measured by using primers RPP0C-Fw-5′-TCTTAGTTGGAATGTTCAGCACCTG-3′, and RPP0C-Rv-5′-CAAGGTTGGAGCCCCTGCTCGTGTT-3′. Real-time PCR was performed on a CFX96 real-time SYBR system (Bio-Rad) using detection of SYBR green according to the Bio-Rad protocol with the following condition: 95 °C for 3 min, 30 cycles of 95 °C for 10 s, 50 °C for 20 s, and 72 °C for 30 s (Salim et al., 2013).

Phylogenetic analysis

Sequence alignments were generated based on a comparison of the amino acid sequences using the ClustalW program (Thompson et al., 1994) with values: 10 for gap opening penalty, 0.1 for gap extension penalty in pairwise alignment, 10 for gap opening penalty, and 0.2 for gap extension penalty in multiple alignment, Gonnet for protein weight matrix, 4 for gap separation distance, residue-specific penalties, hydrophilic penalties, 30% delay divergent cutoff. These alignments were used to construct the neighbor-joining unrooted phylogenetic trees using MEGA 5.1 (Tamura et al., 2011) with scope of all selected taxa, amino acid substitution type following Poisson model, uniform rates, homogenous pattern among lineages, and complete deletion for gaps or missing data treatment. The scale bar of 0.1 indicates to a 10% change and each number shown next to the branches is the percentage of replicate trees in which the related taxa clustered in the bootstrap test with 10,000 replicates.

Acknowledgements

This work was funded by a Discovery grant from the National Sciences and Engineering Research Council of Canada and by a Canada Research Chair in Plant Biotechnology to V.D.L. We also acknowledge funding by Genome Canada, Genome Alberta, Genome Prairie, Genome Quebec, Genome British Columbia, the Canada Foundation for Innovation, the Ontario Ministry of Research and Innovation, the National Research Council of Canada, and other government and private sector partners. We thank Dr. Peter Facchini (University of Calgary, Canada) for providing the VIGS vectors, and Dr. Dae Kyun Ro (University of Calgary, Canada) for providing the yeast expression system. We are also grateful to Dr. Sarah O′Connor (The John Innes Center, UK) and Dr. John Pickett (Rothamsted Experimental Station, UK) for the synthesis of iridodial, and Dr. Hajime Mizukami (Nagoya City University, Japan) for providing 7-deoxyloganetic acid. We also thank Dr. David Nelson (University of Tennessee, USA) for classifying CYP76A26. We acknowledge the skilled technical work of next generation sequencing personnel at the McGill University-Genome Québec-Innovation Centre (Canada). We also thank Christopher Sensen, Mei Xiao, and Ye Zhang (University of Calgary, Canada) for their dedicated bioinformatic support and gene annotation efforts that greatly facilitated the practical use of the Phytometasyn website.

Appendix A. Supplementary data

Supplementary data associated with this article can be found, in the online version, at http://dx.doi.org/10.1016/j.phytochem.2014.02.009.

References

Asada, K., Salim, V., Masada-Atsumi, S., Edmunds, E., Nagatoshi, M., Terasaka, K., Mizukami, H., De Luca, V., 2013. A 7-deoxyloganetic acid glucosyltransferase contributes a key step in Secologanin Biosynthesis in Madagascar periwinkle. Plant Cell 25, 4123–4134.

Bradford, M.M., 1976. A rapid and sensitive method for the quantification of microgram quantities of protein utilizing the principle of protein–dye binding. Anal. Biochem. 72, 248–254.

Burch-Smith, T.M., Anderson, J.C., Martin, G.B., Dinesh-Kumar, S.P., 2004. Applications and advantages of virus-induced gene silencing for gene function studies in plants. Plant J. 39, 734–746.

Burlat, V., Oudin, A., Courtois, M., Rideau, M., St-Pierre, B., 2004. Co-expression of three MEP pathway genes and geraniol 10-hydroxylase in internal phloem parenchyma of *Catharanthus roseus* implicates multicellular translocation of intermediates during the biosynthesis of monoterpene indole alkaloids and isoprenoid-derived primary metabolites. Plant J. 38, 131–141.

Collu, G., Unver, N., Peltenburg-Looman, A.M., van der Heijden, R., Verpoorte, R., Memelink, J., 2001. Geraniol 10-hydroxylase, a cytochrome P450 enzyme involved in terpenoid indole alkaloid biosynthesis. FEBS Lett. 508, 215–220.

De Luca, V., Salim, V., Levac, D., Atsumi, S.M., Yu, F., 2012. Discovery and functional analysis of monoterpenoid indole alkaloid pathways in plants. Methods Enzymol. 515, 207–229.

Dinda, B., Debnath, S., Harigaya, Y., 2007. Naturally occurring iridoids. A review, Part 1. Chem. Pharm. Bull. 55, 159–222.

Dinda, B., Debnath, S., Banik, R., 2011. Naturally occurring iridoids and secoiridoids. An updated review, Part 4. Chem. Pharm. Bull. 59, 803–833.

Dinesh-Kumar, S.P., Anandalakshmi, R., Marathe, R., Schiff, M., Liu, Y., 2003. Virus-induced gene silencing. Methods Mol. Biol. 236, 287–294.

El-Sayed, M., Verpoorte, R., 2007. *Catharanthus* terpenoid indole alkaloids: biosynthesis and regulation. Phytochem. Rev. 6, 277–305.

Facchini, P.J., Bohlmann, J., Covello, P.S., De Luca, V., Mahadevan, R., Page, J.E., Ro, D.K., Sensen, C.W., Storms, R., Martin, V.J., 2012. Synthetic biosystems for the production of high-value plant metabolites. Trends Biotechnol. 30, 127–131.

Geu-Flores, F., Sherden, N.H., Courdavault, V., Burlat, V., Glenn, W.S., Wu, C., Nims, E., Cui, Y., O'Connor, S.E., 2012. An alternative route to cyclic terpenes by reductive cyclization in iridoid biosynthesis. Nature 492, 138–142.

Giddings, L.A., Liscombe, D.K., Hamilton, J.P., Childs, K.L., DellaPenna, D., Buell, C.R., O'Connor, S.E., 2011. A stereoselective hydroxylation step of alkaloid biosynthesis by a unique cytochrome P450 in *Catharanthus roseus*. J. Biol. Chem. 286, 16751–16757.

Gietz, D., St. Jean, A., Woods, R.A., Schiestl, R.H., 1992. Improved method for high efficiency transformation in intact yeast cells. Nucleic Acids Res. 20, 1425.

Góngora-Castillo, E., Childs, K.L., Fedewa, G., Hamilton, J.P., Liscombe, D.K., Magallanes-Lundback, M., Mandadi, K.K., Nims, E., Runguphan, W., Vaillancourt, B., Varbanova-Herde, M., Dellapenna, D., McKnight, T.D., O'Connor, S., Buell, C.R., 2012a. Development of transcriptomic resources for interrogating the biosynthesis of monoterpene indole alkaloids in medicinal plant species. PLoS One 7, e52506.

Góngora-Castillo, E., Fedewa, G., Yeo, Y., Chappell, J., DellaPenna, D., Buell, C.R., 2012b. Genomic approaches for interrogating the biochemistry of medicinal plant species. Methods Enzymol. 517, 139–159.

Guirimand, G., Guihur, A., Ginis, O., Poutrain, P., Héricourt, F., Oudin, A., Lanoue, A., St-Pierre, B., Burlat, V., Courdavault, V., 2011. The subcellular organization of strictosidine biosynthesis in *Catharanthus roseus* epidermis highlights several trans-tonoplast translocations of intermediate metabolites. FEBS J. 278, 749–763.

Helliwell, C.A., Sheldon, C.C., Olive, M.R., Walker, A.R., Zeevaart, J.A., Peacock, W.J., Dennis, E.S., 1998. Cloning of the Arabidopsis ent-kaurene oxidase gene GA3. Proc. Natl. Acad. Sci. USA 95, 9019–9024.

Helliwell, C.A., Chandler, P.M., Poole, A., Dennis, E.S., Peacock, W.J., 2001. The CYP88A cytochrome P450, ent-kaurenoic acid oxidase, catalyzes three steps of the gibberellin biosynthesis pathway. Proc. Natl. Acad. Sci. USA 98, 2065–2070.

Höfer, R., Dong, L., André, F., Ginglinger, J.F., Lugan, R., Gavira, C., Grec, S., Lang, G., Memelink, J., Van Der Krol, S., Bouwmeester, H., Werck-Reichhart, D., 2013. Geraniol hydroxylase and hydroxygeraniol oxidase activities of the CYP76 family of cytochrome P450 enzymes and potential for engineering the early steps of the (seco)iridoid pathway. Metab. Eng.. http://dx.doi.org/10.1016/j.ymben.2013.08.001i.

Hotze, M., Schröder, G., Schröder, J., 1995. Cinnamate 4-hydroxylase from *Catharanthus roseus* and a strategy for the functional expression of plant cytochrome P_{450} proteins as translational fusions with P_{450} reductase in *Escherichia coli*. FEBS Lett. 374, 345–350.

Laflamme, P., St-Pierre, B., De Luca, V., 2001. Molecular and biochemical analysis of a madagascar periwinkle root-specific minovincinine-19-hydroxy-*O*-acetyltransferase. Plant Physiol. 125, 189–198.

Ikeda, H., Esaki, N., Nakai, S., Hashimoto, K., Uesato, S., Soda, K., Fujita, T., 1991. Acyclic monoterpene primary alcohol: $NADP^+$ oxidoreductase of *Rauwolfia serpentina* cells: the key enzyme in biosynthesis of monoterpene alcohols. J. Biochem. 109, 341–347.

Irmler, S., Schröder, G., St-Pierre, B., Crouch, N.P., Hotze, M., Schmidt, J., Strack, D., Matern, U., Schröder, J., 2000. Indole alkaloid biosynthesis in *Catharanthus roseus*: new enzyme activities and identification of cytochrome P450 *CYP72A1* as secologanin synthase. Plant J. 24, 797–804.

Kaltenbach, M., Schröder, G., Schmelzer, E., Lutz, V., Schröder, J., 1999. Flavonoid hydroxylase from *Catharanthus roseus*: cDNA, heterologous expression, enzyme properties and cell-type specific expression in plants. Plant J. 19, 183–193.

Kawai, H., Kuroyanagi, M., Ueno, A., 1988. Iridoid glucosides from *Lonicera japonica* THUNB. Chem. Pharm. Bull. 36, 3664–3666.

Liscombe, D.K., O'Connor, S.E., 2011. A virus-induced gene silencing approach to understanding alkaloid metabolism in *Catharanthus roseus*. Phytochemistry 72, 1969–1977.

Magnotta, M., Murata, J., Chen, J., De Luca, V., 2007. Expression of deacetylvindoline-4-*O*-acetyltransferase in *Catharanthus roseus* hairy roots. Phytochemistry 68, 1922–1931.

Murata, J., Roepke, J., Gordon, H., De Luca, V., 2008. The leaf epidermome of *Catharanthus roseus* reveals its biochemical specialization. Plant Cell 20, 524–542.

Mizutani, M., Sato, F., 2011. Unusual P450 reactions in plant secondary metabolism. Arch. Biochem. Biophys. 507, 194–203.

O'Connor, S.E., Maresh, J.J., 2006. Chemistry and biology of monoterpene indole alkaloid biosynthesis. Nat. Prod. Rep. 23, 532–547.

Oudin, A., Courtois, M., Rideau, M., Clastre, M., 2007. The iridoid pathway in *Catharanthus roseus* alkaloid biosynthesis. Phytochem. Rev. 6, 259–276.

Pompon, D., Louerat, B., Bronine, A., Urban, P., 1996. Yeast expression of animal and plant P450s in optimized redox environments. Methods Enzymol. 272, 51–64.

Ro, D.K., Ehlting, J., Douglas, C.J., 2002. Cloning, functional expression, and subcellular localization of multiple NADPH-cytochrome P450 reductases from hybrid poplar. Plant Physiol. 130, 1837–1851.

Ro, D.K., Paradise, E.M., Ouellet, M., Fisher, K.J., Newman, K.L., 2006. Production of the antimalarial drug precursor artermisinic acid in engineered yeast. Nature 440, 940–943.

Ro, D.K., Ouellet, M., Paradise, E.M., Burd, H., Eng, D., Paddon, C.J., Newman, J.D., Keasling, J.D., 2008. Induction of multiple pleiotropic drug resistance genes in yeast engineered to produce an increased level of anti-malarial drug precursor, artemisinic acid. BMC Technol. 8, 83.

Roepke, J., Salim, V., Wu, M., Thamm, A.M., Murata, J., Ploss, K., Boland, W., De Luca, V., 2010. Vinca drug components accumulate exclusively in leaf exudates of Madagascar periwinkle. Proc. Natl. Acad. Sci. 107, 15287–15292.

Salim, V., De Luca, V., 2013. Towards complete elucidation of monoterpene indole alkaloid biosynthesis pathway: *Catharanthus roseus* as a pioneer system. Adv. Bot. Res. 68, 1–37.

Salim, V., Yu, F., Altarejos-Caballero, J., De Luca, V., 2013. Virus induced gene silencing identifies *Catharanthus roseus* 7-deoxyloganic acid 7-hydroxylase, a step in iridoid and monoterpenoid indole alkaloid biosynthesis. Plant J.. http://dx.doi.org/10.1111/tpj.12330.

Schröder, G., Unterbusch, E., Kaltenbach, M., Schmidt, J., Strack, D., De Luca, V., Schröder, J., 1999. Light-induced cytochrome P450-dependent enzyme in indole alkaloid biosynthesis: tabersonine 16-hydroxylase. FEBS Lett. 458, 97–102.

Simkin, A.J., Miettinen, K., Claudel, P., Burlat, V., Guirimand, G., Courdavault, V., Papon, N., Meyer, S., Godet, S., St-Pierre, B., Giglioli-Guivarc'h, N., Fischer, M.J.C., Memelink, J., Clastre, M., 2013. Characterization of the plastidial geraniol synthase from Madagascar periwinkle which initiates the monoterpenoid branch of the alkaloid pathway in internal phloem associated parenchyma. Phytochemistry 85, 36–43.

Sung, P.H., Huang, F.C., Do, Y.Y., Huang, P.L., 2011. Functional expression of geraniol 10-hydroxylase reveals its dual function in the biosynthesis of terpenoid and phenylpropanoid. J. Agric. Food Chem. 59, 4637–4643.

Tamura, K., Peterson, D., Peterson, N., Stecher, G., Nei, M., Kumar, S., 2011. MEGA5: molecular evolutionary genetics analysis using maximum likelihood, evolutionary distance, and maximum parsimony methods. Mol. Biol. Evol. 28, 2731–2739.

Teoh, K.H., Polichuk, D.R., Reed, D.W., Nowak, G., Covello, P.S., 2006. *Artemisia annua* (Asteraceae) trichome-specific cDNAs reveal CYP71AV1, a cytochrome P450 with a key role in the biosynthesis of the antimalarial sesquiterpene lactone artermisinin. FEBS Lett. 580, 1411–1416.

Thompson, J.D., Higgins, D.G., Gibson, T.J., 1994. CLUSTALW: Improving the sensitivity of progressive multiple sequence alignment through sequence weighting, position-specific gap penalties and weight matrix choice. Nucleic Acids Res. 22, 4673–4680.

Uesato, S., Miyauchi, M., Itoh, H., Inouye, H., 1986. Biosynthesis of iridoid glucosides in *Galium mollugo*, *G. spurium* var *Echinospermon* and *Deutzia crenata*, intermediacy of deoxyloganic acid, loganin, and iridodial glucoside. Phytochemistry 25, 2515–2521.

Van der Heijden, R., Jacobs, D.I., Snoeijer, W., Hallard, D., Verpoorte, R., 2004. The *Catharanthus* alkaloids: pharmacognosy and biotechnology. Curr. Med. Chem. 11, 607–628.

Van Moerkercke, A., Fabris, M., Pollier, J., Baart, G.J., Rombauts, S., Hasnain, G., Rischer, H., Memelink, J., Oksman-Caldentey, K.M., Goossens, A., 2013. CathaCyc, a metabolic pathway database built from Catharanthus roseus RNA-Seq data. Plant Cell Physiol. 54, 673–685.

Xiao, M., Zhang, Y., Chen, X., Lee, E.J., Barber, C.J., Chakrabarty, R., Desgagné-Penix, I., Haslam, T.M., Kim, Y.B., Liu, E., MacNevin, G., Masada-Atsumi, S., Reed, D., Stout, J.M., Zerbe, P., Zhang, Y., Bohlmann, J., Covello, P.S., De Luca, V., Page, J.E., Ro, D.K., Martin, V.J.J., Facchini, P.J., Sensen, C.W., 2013. Transcriptome analysis based on next-generation sequencing of non-model plants producing specialized metabolites of biotechnological interest. J. Biotechnol. 166, 122–134.